Finite Element Models of Neuron Electrode Sealing Interfaces

Charles T. M. Choi[1,2] and Shan-Jen You[3]

[1]Department of Computer Science and Institute of Biomedical Engineering, National Chiao Tung University, Taiwan, R.O.C.
[2]Department of Electrical Engineering, National Chiao Tung University, Taiwan, R.O.C.
[3]Department of Electrical Engineering, I-Shou University, Kaohsiung, Taiwan, R.O.C.

It is desirable to detect any leakage current when microelectrode is used to stimulate a neuron electrically. This paper proposes a new approach to study the neuron-electrode sealing interface problem. As opposite to the traditional bi-domain FEM that need a two-step process of indirect coupling of two domains with a circuit equation, which involves solving a set of ordinary differential equation, this paper proposed a more elegant approach to study the neuron-electrode sealing interface problem based on a single domain finite element model. The result shows the stimulation electrical potential distribution and the sealing resistance match the published simulation and experimental results.

Index Terms—**Bio-electric problem, finite element model, neuron-electrode interface, sealing resistance.**

I. Introduction

THE quality of the electrical contact between a cultured neuron and a substrate embedded microelectrode is important for the effective transfer of an extracellular applied stimulus current to the intracellular potential [1]–[4]. When using a microelectrode to stimulate a neuron electrically, it is desirable to maximize the current transfer from the input electrode to the neuron which is typically covered fully by an electrode through a neuron-electrode interface. Typically, there are gaps between the cell membrane and the substrate (Fig. 1). The gap allows the leakage current to get out and lowers the stimulation efficiency of such a system (Fig. 1). The leakage current is affected by the sealing resistance. The geometry of the neuron-electrode interface is also influenced by the sealing resistance. Previous studies were based on equivalent circuit models which did not take into account the geometries of the neuron and electrode [1]. More recently, a bi-domain finite element-circuit model [1], [5], [6] has been developed which characterizes the neuron membrane as resistors between intracellular (inside the neuron) and extracellular (outside the neuron) domains. While this approach is an improvement over the equivalent circuit model, it is complicated to insert resistors into finite element models. The proposed method characterizes the neuron membrane by adding a layer in a finite element model of the neuron-electrode interface. This reduces the complexity of the finite element (FE) model of the neuron-electrode and allows accurate modeling of the neuron-electrode interface.

II. Method

The neuron electrode interface model is shown in Fig. 1 [5]. The input current flow from the electrode $(\mathrm{I_{stim}})$ is separated into two branches: the leakage current $(\mathrm{I_{seal}})$ and current through the cell $(\mathrm{I_{cell}})$. In these circuits, the membrane is split into an upper part and a lower part over the sealing gap and defined as the free membrane and the junction membrane,

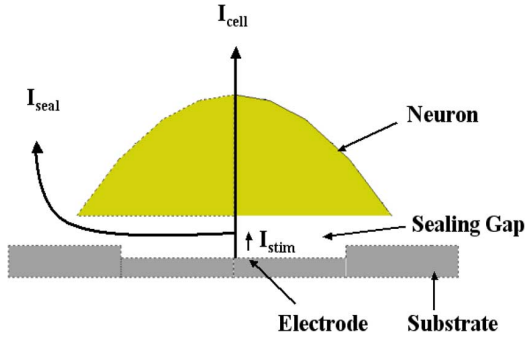

Fig. 1. Definition of neural electrode interface model [5].

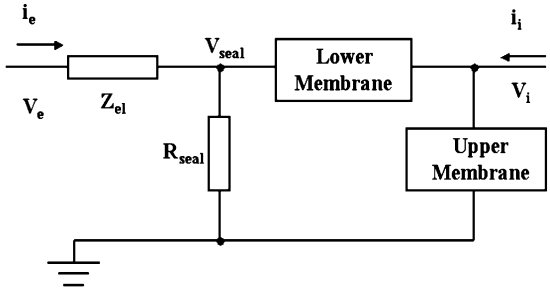

Fig. 2. Equivalent circuit of the neuron-electrode interface [5].

respectively, as shown in Fig. 2 [6]. The electrode-electrolyte interface and the sealing resistance are represented by a single component. In Fig. 3, a coupled circuit and bi-domain finite element model [5] is an improvement of the equivalent circuit model (Fig. 2). In the bi-domain model, the Poisson equation was solved in the extracellular domain and the intracellular domain separately as static problems. At the boundary nodes of the intracellular domain and the extracellular domain, the nodal potentials were extracted and the Ohm's law equation was applied:

$$\phi_{mem,n} = i_{mem,n} \cdot R_{mem,n} \tag{1}$$

where $\phi_{mem,n}$ is the membrane potential, $i_{mem,n}$ is the membrane current, $R_{mem,n}$ is the resistance between node n at the membrane border of the extracellular and intracellular domain. This approach is equivalent to inserting a resistor between the extracellular and intracellular domain in each border node to represent the membrane (Fig. 3) [5].

Regarding the time domain problem, the Poisson equation is solved in the two domains separately. The nodal potentials at

Manuscript received July 08, 2011; revised October 12, 2011; accepted October 21, 2011. Date of current version January 25, 2012. Corresponding author: C. T. Choi (e-mail: c.t.choi@ieee.org).

Color versions of one or more of the figures in this paper are available online at http://ieeexplore.ieee.org.

Digital Object Identifier 10.1109/TMAG.2011.2175717

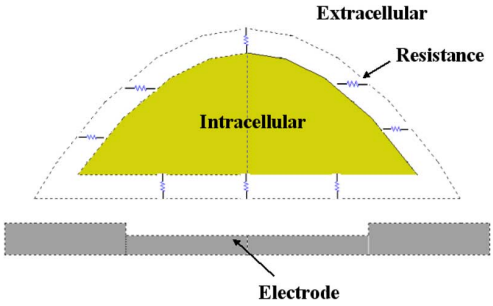

Fig. 3. A finite element model of a neuron and an electrode is shown. The neuron membrane is represented by resistors [5].

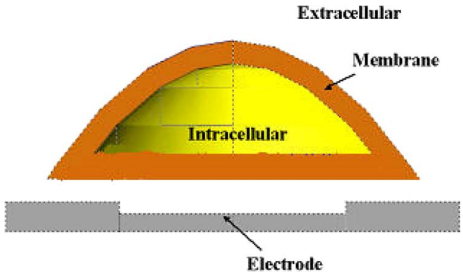

Fig. 4. A model of neuron-electrode interface by modeling the neuron membrane as a finite element layer. The result from a dense FE mesh with 300,000 nodes has been compared with the result from a coarse FE mesh with 25,000 nodes for convergence and accuracy.

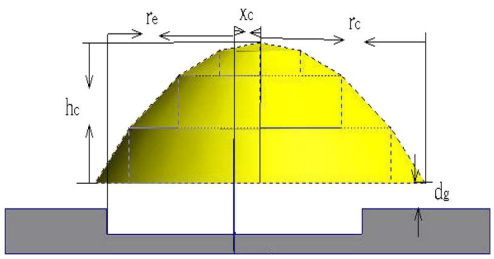

Fig. 5. Geometry of the neuron-electrode interface for parametric study [5].

the membrane border were extracted and the following ordinary differential equation (ODE) was solved [6]:

$$\frac{d}{dt}\phi_{mem,n} = \frac{i_{mem,n} - \phi_{mem,n}/R_{mem,n}}{C_{mem,n}} \tag{2}$$

where $C_{mem,n}$ represents the membrane capacitance.

This approach is complicated due to the difference in the finite element and the circuit formulations.

A. Proposed Interface Layer

As shown in Fig. 4, instead of using resistors to represent the real neuron membrane, the proposed method uses an anisotropic layer which allows the current to get in or out of the neuron perpendicularly to the membrane to represent the real neuron membrane.

A resistance is used to model the electrical characteristic of the neuron membranes in [5]. In [6], a set of differential equations is used to characterize the membrane electrically. This set of differential equations can be represented by a membrane resistance and a shunt membrane capacitance. In this interface model, an interface layer is inserted between extracellular and intracellular domains to represent the neuron membrane. Since a passive model of the neuronal membrane is assumed here, only a resistance and a capacitance are incorporated in this layer.

The neuron membrane resistance (R_{mem}) can be computed as:

$$R_{mem} = \frac{1}{A\sigma_{mem}} \tag{3}$$

where σ_{mem} is the conductivity of the membrane per unit area; $\sigma_{mem} = 0.3\,\mathrm{mS/cm^2}$ [5], and A is the membrane area. Resistance, R_{mem}, can also be written as:

$$R_{mem} = \frac{\ell}{\sigma A} \tag{4}$$

where ℓ is the distance between extracellular and intracellular domains, and σ is the conductivity of the interface. By equating (3) and (4) and simplifying:

$$\sigma = \sigma_{mem} \cdot \ell \tag{5}$$

where $\ell = 0.3\,\mu\mathrm{m}$ in this model, an interface layer conductivity $\sigma = 0.9\ \mu\mathrm{S/m}$ is obtained.

Next, a membrane capacitance C_{mem} is also incorporated in the membrane layer in the current method.

$$C_{mem} = c_{mem} \cdot A \tag{6}$$

where C_{mem} is the total capacitance of the membrane and c_{mem} is the membrane capacitance per unit area, $c_{mem} = 1\ \mu\mathrm{F/cm^2}$ [6]. The capacitance of the membrane layer can be computed as:

$$C_{mem} = \frac{\varepsilon_{mem} A}{\ell} \tag{7}$$

where ε is the permittivity used to model the capacitance for the membrane. By equating (6) and (7) and simplifying:

$$\varepsilon_{mem} = c_{mem} \cdot \ell \tag{8}$$

and $\varepsilon_{mem} = 3 \times 10^{-9}\ \mathrm{F/m}$. The σ and ε_{mem} can be used to form the anisotropic layer, which represents the membrane.

B. Seal Resistance and Membrane Depolarization Studies

Next, the sealing resistance is studied using parameters as shown in Fig. 5 and the lumped circuit model (LCM) as shown in Fig. 6. The circuit model is divided into three resistive components (Fig. 6): the sealing resistance and the upper and lower membrane resistances. When the neuron is centered on the electrode $(x_c = 0)$, the geometry parameters can be used for computing the circuit components [5]:

$$R_{seal} = \frac{1}{2\pi \cdot d_g \cdot \sigma_{medium}} \ln\left(\frac{r_c}{r_e}\right) \tag{9}$$

$$R_{low} = \frac{1}{\pi \cdot \sigma_{mem} \cdot r_e^2} \tag{10}$$

$$R_{up} = \frac{1}{\pi \cdot \sigma_{mem} \cdot f(h_c) \cdot r_c^2} \tag{11}$$

where $\sigma_{medium} = 1.65\ (\mathrm{S/m})$ and $f(h_c) = 1.43$.

The depolarization of the upper membrane due to a stimulus current through the electrode for the LCM can be written as:

$$V_{up} = R_{seal} \frac{R_{up}}{R_{seal} + R_{low} + R_{up}} \cdot I_{stim}. \tag{12}$$

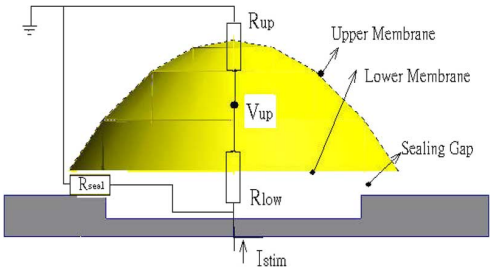

Fig. 6. A circuit model of the neuron-electrode interface. The electrode impedance is left out of the model and only resistive membrane properties are modeled [5].

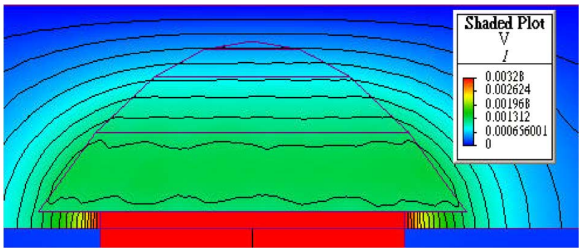

Fig. 7. For a completely sealed neuron-electrode interface, a 1 nA stimulation current generates a $\mathrm{R_{seal}}$ of 3.28 $\mathrm{M\Omega}$, which is identical to bi-domain FE modeling results and consistent with the experimental value of $4\mathrm{M\Omega}$ [5]. The contour shown above is in volt.

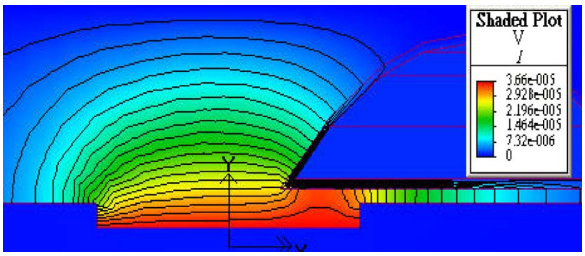

Fig. 8. For an incomplete seal between the neuron and the electrode, a 1 nA stimulation current generates a Rseal of 36.6 kΩ, which is consistent with the bi-domain FE modeling results [5]. The contour shown above is in volt.

III. Result

In Fig. 7, the computed potential distribution due to a 1 nA stimulus current is depicted in a cross section of the model. The equipotential lines in the medium are marked by the boundaries between two adjacent colored regions. At complete sealing (Fig. 7), the equipotential lines are concentrated in the sealing gap, which indicates a potential drop over the sealing gap. A maximum depolarization of 1.02 mV (stimulus transfer) occurs at the upper membrane, and a hyperpolarization of 2.25 mV occurs at the lower membrane. When the sealing is defective as shown in Fig. 8, the equipotential lines are spread upward more widely, which indicates a leakage current in the medium. The changes in membrane potential are reduced to the microvolt range. From the electrode potential V_e, and the stimulus current at the center, a sealing resistance of 3.28 $\mathrm{M\Omega}$ is computed from the results (Fig. 7). As shown in Fig. 8, a sealing resistance of only 36.6 kΩ is computed when the sealing is defective. These results reveal that the sealing resistance is strongly related to the stimulus transfer. The transition from complete to defective sealing causes a drastic decrease in both the stimulus transfer and the sealing resistance. The finite element models have been validated for numerical accuracy through convergence studies with a dense finite element mesh and a coarse mesh (Fig. 4).

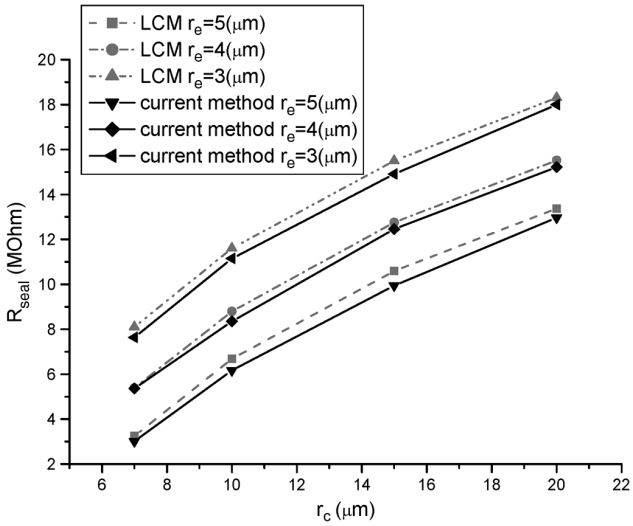

Fig. 9. Simulation results from the lumped circuit model (eq. (9)). Sealing resistance, plotted versus the radius of the neuron while the radius of the electrode is varied ($r_e = 5\ \mu\mathrm{m}$, $r_e = 4\ \mu\mathrm{m}$, $r_e = 3\ \mu\mathrm{m}$).

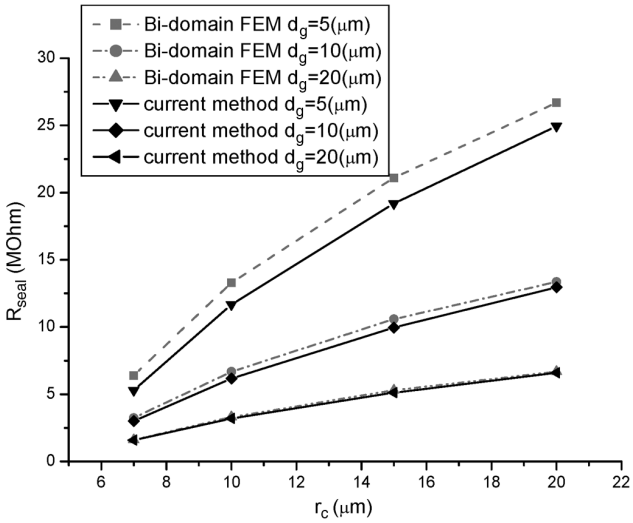

Fig. 10. The simulation results from bi-domain finite element model [5]. Sealing resistance, plotted versus the radius of the neuron while the thickness of the sealing gap is varied ($d_g = 5\ \mu\mathrm{m}$, $d_g = 10\ \mu\mathrm{m}$, $d_g = 20\ \mu\mathrm{m}$).

In Figs. 9 and 10, the sealing resistance is examined by varying the sealing gap, the radius of the electrode and the radius of the neuron. Fig. 9 shows the sealing resistance as a function of the neuronal radius and electrode radius change. The sealing resistance increases with the increase of the neuronal radius. On the other hand, the sealing resistance decreases with increase of the electrode radius. The current method shows similar results to the LCM results (Fig. 9). Similarly, the sealing resistance increases with the increase of the neuronal radius (Fig. 10), and the results of the bi-domain FEM solution versus the proposed FEM method are compared. The proposed FEM approach tracks the bi-domain FEM solution quite well. The sealing resistance increases with decrease of the sealing gap, which is consistent with the resistance formula (9).

Figs. 11–13 show the depolarization potential of the upper membrane (Fig. 6). The current (or proposed) method matches the bi-domain FEM results in both Figs. 11, 12. The depolarization potential is proportional to the radius of the neuron. It is inversely proportional to the electrode radius as well as the

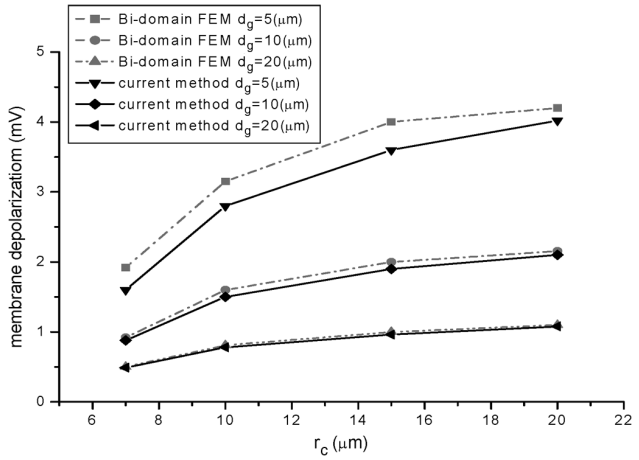

Fig. 11. Simulation results from the Bi-domain finite element model [5]. Membrane depolarization, plotted versus the radius of the neuron while the thickness of the sealing gap is varied ($d_g = 5\ \mu\mathrm{m}$, $d_g = 10\ \mu\mathrm{m}$, $d_g = 20\ \mu\mathrm{m}$).

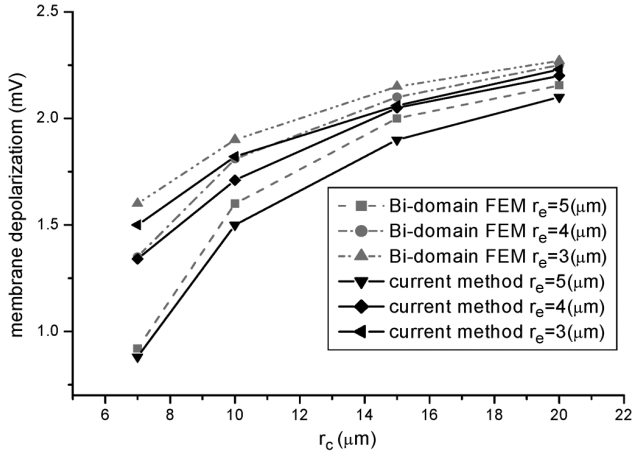

Fig. 12. Simulation results from the finite element model [5]. Membrane depolarization, plotted versus the radius of the neuron while the radius of the electrode is varied ($r_e = 5\ \mu\mathrm{m}$, $r_e = 4\ \mu\mathrm{m}$, $r_e = 3\ \mu\mathrm{m}$).

sealing gap. However, the results from the LCM do not resemble the results from the current (or proposed) method (Fig. 13) or the bi-domain FEM (not shown for brevity). This is due to the fact that LCM does not take into account the current going into the lower membrane in the vicinity of the sealing gap. LCM assumes all the currents penetrating the neuron directly through the center portion of the neuron. In short, the LCM does not take into account any geometric variations of the model, and thus the error shown in Fig. 13. While the static problem is solved here, the time domain problem can be solved (not shown) with the proposed interface to generate an approximated response based on passive models.

Since the FE domains of the proposed method and the traditional method are very similar in size, the CPU time required for the proposed method is similar to the traditional method. A limitation of the proposed model is that it does not take into account of other properties such as hydrophilic/hydrophobic coating for electrode.

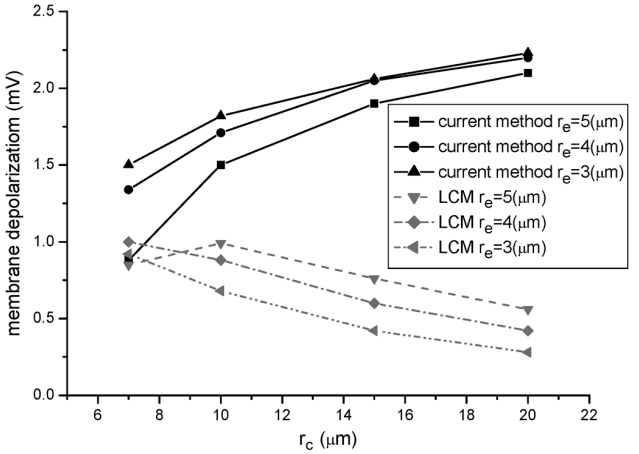

Fig. 13. Simulation results from lumped circuit model (eq. (12)). Membrane depolarization, plotted versus the radius of the neuron while the radius of the electrode is varied ($r_e = 5\ \mu\mathrm{m}$, $r_e = 4\ \mu\mathrm{m}$, $r_e = 3\ \mu\mathrm{m}$).

IV. Conclusion

This paper proposes to use an interface layer approach to solve the neuron-electrode interface stimulation problem using a finite element model. The traditional bi-domain FEM requires a 2-step process of indirect coupling with a circuit equation, which involves solving a set of ODE. The proposed method saves pre-processing time while maintaining a comparable solution accuracy.

Acknowledgment

This research was supported in part by National Science Council, R.O.C. (98-2221-E-009-089 MY3), (99-2321-B-009-001-) and (100-2321-B-009-002-).

References

[1] J. R. Buitenweg, W. L. C. Rutten, and E. Marani, "Finite element modeling of the neuron-electrode interface: Sealing resistance and stimulus transfer at transitions from complete to defect sealing," *IEEE Eng. Med. Biol. Soc. Mag.*, vol. 6, pp. 2854–2857, Oct.–Nov. 1998.

[2] S. Martinoia, P. Massobrio, M. Bove, and G. Massobrio, "Cultured neurons coupled to microelectrode arrays: Circuit models, simulations and experimental data," *IEEE Trans. Biomed. Eng.*, vol. 51, no. 5, pp. 859–864, May 2004.

[3] D. A. Robinson, "The electrical properties of metal microelectrodes," *Proc. IEEE*, vol. 56, pp. 1065–1071, 1968.

[4] J. Lin, X. Wu, P. Huang, T. Ren, and L. Liu, "A 16-site neural recording probe array and its circuit model simulation," in *2005 First Int. Conf. Neural Interface and Control Proc.*, May 2005, pp. 68–71.

[5] J. R. Buitenweg, W. L. C. Rutten, and E. Marani, "Finite element modeling of the neuron-electrode interface: A valuable tool for studying and optimizing the neuron-electrode contact," *IEEE Med. Biol. Soc. Mag.*, vol. 19, pp. 46–52, Nov.–Dec. 2000.

[6] J. R. Buitenweg, W. L. C. Rutten, and E. Marani, "Geometry-based finite-element modeling of the electrical contact between a cultured neuron and a microelectrode," *IEEE Trans. Biomed. Eng.*, vol. 50, no. 4, pp. 501–509, Apr. 2003.